BJR

https://doi.org/10.1259/bjr.20170414

Received: 04 June 2017 | Revised: 10 November 2017 | Accepted: 17 November 2017

Cite this article as:
Wu W, Niu Y, Kong X, Liu D, Long X, Shu S, et al. Application of diffusion tensor imaging in quantitatively monitoring chronic constriction injury of rabbit sciatic nerves: correlation with histological and functional changes. *Br J Radiol* 2017; **90**: 20170414.

FULL PAPER

Application of diffusion tensor imaging in quantitatively monitoring chronic constriction injury of rabbit sciatic nerves: correlation with histological and functional changes

[1]WENJUN WU, [2]YANFENG NIU, [1]XIANGQUAN KONG, [1]DINGXI LIU, [1]XI LONG, [1]SHENGLEI SHU, [1]XIAOYUN SU, [1]BING WANG, [1]XIAOMING LIU, [1]YAMEI MA and [1]LIXIA WANG

[1]Department of Radiology, Union Hospital, Tongji Medical College, Huazhong University of Science and Technology, Wuhan, China
[2]Department of Gastrointestinal Surgery, Union Hospital, Tongji Medical College, Huazhong University of Science and Technology, Wuhan, China

Address correspondence to:
Xiangquan Kong
E-mail: *kxqwuhan@163.com*
Lixia Wang
E-mail: *wanglixiawuhan@outlook.com*

The authors Wenjun Wu and Yanfeng Niu contributed equally to the work

Objective: To investigate the potential of diffusion tensor imaging (DTI) in quantitatively monitoring chronic constriction injuri (CCI) of sciatic nerves and to analyse the association of DTI parameters with nerve histology and limb function.
Methods: CCI was created on sciatic nerves in the right hind legs of 20 rabbits with the left as control. DTI parameters—fractional anisotropy (FA), apparent diffusion coefficient (ADC), axial diffusivity (AD) and radial diffusivity (RD)—and limb function were longitudinally evaluated. Pathology analysis was performed on day 3 (d3), week 1 (w1), 2, 4, 6, 8 and 10.
Results: FA of the constricted nerves decreased on d3 (0.316 3 0.044) and increased from w1 to w10 (0.331 3 0.018, 0.354 3 0.044, 0.375 3 0.015, 0.394 3 0.020, 0.42 3 0.03 and 0.464 3 0.039). ADC increased on d3 until w2 (1.502 3 0.126, 1.462 3 0.058 and 1.473 3 0.124 × 10^{-3} mm^2 s^{-1}) and decreased to normal from w4 to w10 (1.356 3 0.129, 1.375 3 0.107, 1.290 3 0.064 and 1.298 3 0.026 × 10^{-3} mm^2 s^{-1}). AD decreased and stayed low from d3 to w10 (2.042 3 0.160, 2.005 3 0.095, 2.057 3 0.124, 1.952 3 0.213, 1.988 3 0.180, 1.947 3 0.106 and 2.097 3 0.114). RD increased on d3 (1.233 3 0.152) and declined from w1 to w10 (1.19 3 0.06, 1.181 3 0.14, 1.071 3 0.102, 1.068 3 0.084, 0.961 3 0.063 and 0.923 3 0.058). FA, ADC and RD correlated significantly with limb functional scores (all Ps < 0.0001) and their changes were associated with histological changes.
Conclusion: FA, ADC and RD are promising to monitor CCI. AD may be a stable indicator for injury. Histological changes, oedema, axon loss and demyelination, and fibrosis, accompanied the changes of these parameters.
Advances in knowledge: DTI parameters can detect and monitor acute and chronic changes after nerve compression.

INTRODUCTION

Nerve compression syndrome (NCS) is one of the most common forms of peripheral nerve injury. A variety of nerves are susceptible to chronic injuries because of their structural abnormalities. Chronic compression, or entrapment of nerves, induces some common symptoms such as paresthesia, pain and numbness of the limbs. Clinical diagnoses and prognosis assessment of NCS mainly depend on physical examination and electrophysiological experiments.[1,2] However, these methods are highly dependent on the experience of clinicians. Additionally, both are only used for the functional assessment of nerves. Therefore, for accurate diagnoses and treatment, an objective method that can be used to evaluate the structure of peripheral nerves needs to be developed.

Diffusion tensor imaging (DTI) has been widely used in the central nervous system for its quantitative assessment of the diffusion anisotropy of the brain and spinal cord.[3,4] It recently rose to be a promising method in detecting

and monitoring lesions to the peripheral nervous system for its potential to depict the microstructure of nerves.[5,6] Several clinical studies were carried out on the application of DTI in diagnosing NCS, especially the carpal tunnel syndrome (CTS). These studies demonstrated the diagnostic value of the DTI parameters, *e.g.* the fractional anisotropy (FA) value decreased and the values of apparent diffusion coefficient (ADC) and radial diffusivity (RD) increased in patients with CTS compared to the control subjects,[7] FA and ADC values recovered after carpal tunnel release,[8] FA and ADC correlated with electrophysiological measurements and functional assessment,[9] and a proper cutoff value of FA and ADC added the diagnostic accuracy of CTS.[10] Additionally, a study on recurrent CTS demonstrated that axial diffusivity (AD), ADC and RD values decreased along the involved median nerve, while FA increased.[11] Furthermore, animal studies on monitoring acute injuries such as crush injury[12] and traction injury[13] to sciatic nerves using DTI methods reported decreased FA and increased RD after injuries and good correlation between functional changes and the DTI parameters. However, no significant changes of the ADC or AD value were found in previous animal models. Nor were the results of animal studies on acute injuries in accordance with those of clinical studies on NCS.

The present animal models all generate acute degeneration, not continuous stimulation, on nerve fibres, so they are appropriate for studying nerve regeneration, but not for NCS.[12–14] Thus a new animal model is needed to simulate chronic procedures, such as permanent or recurrent compression, entrapment of abnormal skeletal and muscular structure, and adhesion of fibrous tissues, in order to study NCS. Meanwhile, using DTI methods to study an animal model mimicking NCS has never been reported, including the longitudinal changes of DTI parameters and their correlation with functional and pathological changes.

In this study, the chronic constriction injury (CCI) model was used to simulate NCS. The purpose was to investigate the validity of DTI to evaluate CCI to sciatic nerves of rabbits by comparing the DTI parameters with limb functional assessment and pathological changes.

METHODS AND MATERIALS

Subjects

All the animals were used in accordance with the procedures of the Health Guide for the Care and Use of Laboratory Animals and approved by the Institutional Animal Use and Care Committee. 20 Japanese white rabbits, aged at 6–9 months, were provided by the Laboratory Animal Center of Tongji Medical College. Their weight ranged at 2.0–2.2 kg at the beginning and 3.0–3.5 kg at the end of the study. The sciatic nerves in the right hind limbs were selected to have CCI, and the matching nerves on the left side had sham operation. MR imaging and functional assessment were performed longitudinally on six rabbits before and after CCI, and the scanning was performed right before CCI (baseline), day 3, weeks 1, 2, 4, 6, 8 and 10 after the injury. Among the other 14, two were randomly sacrificed for histological evaluation at each of the following time points, day 3, weeks 1, 2, 4, 6, 8, and 10 after injury.

Animal model

The rabbits were anesthetized through intraperitoneal injection of chloral hydrate (10%, 3–3.5 mg kg^{-1}), and the hind limbs were locally anesthetized using lidocaine. The surgery was performed according to the method described by Bennett and Xie[15]. A longitudinal incision was made at the midthigh level and the sciatic nerve was exposed by blunt dissection through biceps femoris. Proximal to the sciatica's trifurcation, the nerve was freed from the adhering tissue and 4 ligatures (4–0 non-absorbable silk suture) were tied loosely around it with intervals of about 1–2 mm. The degree of ligation was suitable to induce mild compression on the superficial epineural vasculature and mild, small fasciculations on the limb muscles. The incision was closed in layers. The sham operation on the left side was performed with exposure of the sciatic nerve and direct suture of the incision.

MR image acquisition

MRI was performed at 3.0T scanner (Magnetom TIM Trio; Siemens, Erlangen, Germany) along with a 4-channel coil (Flex large; Siemens, Erlangen, Germany). The rabbits were examined in a lateral position with their right hind limbs overlapping the left. The coil was used to surround both the limbs completely. Serial follow-ups of T_2 weighted images, PD-weighted images, and DTI of the sciatic nerves were acquired. T_2 weighted imaging with fat suppression was performed using short-time inversion recovery sequence [repetition time/echo time (TR/TE), 3800/167 ms; number of signal averages, 2; slice thickness, 2 mm; no intersection gap; acquisition matrix, 128 × 128]. The rabbit sciatic nerve is typically 1–2 mm in diameter, but exceeds 2 mm after constriction due to swelling. The scanning was made at slices of 2 mm as previously described.[13,16] PD-weighted imaging without fat suppression was performed using fast spin-echo sequence (TR/TE, 907/8.53 ms; number of signal averages, 2; slice thickness, 2 mm; no intersection gap; acquisition matrix, 256 × 256). DTI was performed using spin-echo echo planar imaging (TR/TE, 4000/82 ms; number of signal averages, 8; slice thickness, 2 mm; no intersection gap; b value, 0; 1000 s^{-1} mm^2 with 12 diffusion directions; acquisition matrix, 80 × 80). All four sequences were scanned with the same parameter: field of view, 120 × 120 mm.

Morphological assessment and DTI measurement

The morphological and signal changes of both the CCI sciatic nerves and the sham-operated ones were observed and assessed on routine MRI sequences at several time points. DTI data were calculated using the Siemens post-processing workstation. The original data were sent to the workstation and coregistered before diffusion tensor tractography (DTT) was performed. PD-weighted images were fused with the DTI maps to locate the injury, on which the 4 ligatures were shown to be hypointense nodules (Figure 1). Three round regions of interest (ROIs), each measuring 2 mm^2 in size, were drawn on the fusion images between the intervals of the four ligatures involving the whole lesion to obtain FA, ADC, RD and AD, and averages of each value were calculated. The ROIs were completely covered in the FA signals to minimize the partial volume effect. FA was computed with the following formulas:

Figure 1. DTI measurements of the sciatic nerve. The fused map (a) consisted of PD-weighted image (b) and FA map (c). The constriction injury, already visible on the FA map, was shown as four hypointense nodules on the PD-weighted image (thick arrow). Three ROIs were placed on both the constricted side (thick arrows) and its counterpart (thin arrow) on the sham-operated side. DTI, diffusiontensor imaging; FA, fractionalanisotropy; PD, proton density; ROI, region of interest.

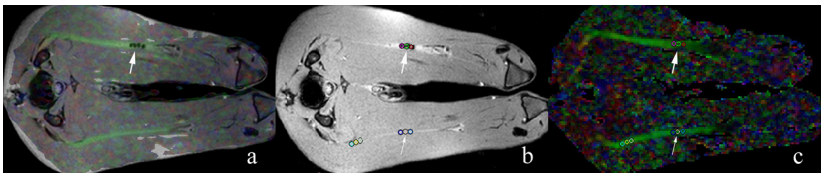

$$\lambda_{||} = \lambda_1 \quad (1)$$

$$\lambda_{\perp} = (\lambda_2 + \lambda_3)/2 \quad (2)$$

$$FA = \sqrt{\frac{3}{2}} \frac{\sqrt{(\lambda_1 - MD)^2 + (\lambda_2 - MD)^2) + \lambda_3 - MD)^2}}{\sqrt{\lambda_1{}^2 + \lambda_2{}^2 + \lambda_3{}^2}} \quad (3)$$

$$\text{mean diffusivity (MD)} = (\lambda_1 + \lambda_2 + \lambda_3)/3 \quad (4)$$

RD and AD values were calculated with the following equations:

$$AD = \lambda_1$$

$$RD = (\lambda_2 + \lambda_3)/2$$

DTT was reconstructed by a multi-ROI method: two ROIs were drawn at both proximal and distal parts of the CCI segment, avoiding the adjacent soft tissues such as fat and muscles. Fibres passing through the two ROIs were produced automatically. The tractographic limit to produce FA measurements was 0.3 and that of the FA angle was 30°, while the minimum fibre length was 10 mm. The DTI measurements and DTT were obtained in the same way on the counterparts of the sham-operated nerves.

Functional assessment

Functional changes of the limbs with injured nerves were evaluated before MR scanning at each time point. The evaluation method was a modified score system based on the Tarlov score and toe-spreading reflex,[12,13] including toe-spreading reflex, response to acupuncture, resistance to hand press and gait. Toe-spreading reflex was evaluated with the following 4-score system: (1) spreading disappeared completely; (2) visible spreading of the 4th or 3rd or 2nd toe; (3) spreading of all three toes but less forceful than normal; (4) normal spreading of three toes. Response to acupuncture was rated with 4 scores: (1) response disappeared completely; (2) small tremor of hind limb to acupuncture, without withdrawing; (3) slower withdrawing of hind limb to acupuncture than normal; (4) response to acupuncture as normal. Resistance to hand press: (1) no resistance; (2) hind limb visibly counteracted hand press; (3) resistance present, but less forceful than normal; (4) normal resistance. Gait scores: (1) complete paralysis of the hind limb; (2) the injured hind limb trail behind the other; (3) normal. The total full score was 15.

Histological examination

Two rabbits were sacrificed randomly by injecting sodium pentobarbital through ear vein at each time point. The injured segment of the nerves and the corresponding part of the sham-operation side were dissected in a length of about 1 cm, fixed in 4% paraformaldehyde, dehydrated through a series of increasing alcohol concentrations, and embedded in paraffin. Paraffin sections were made and haematoxylin–eosin staining, Luxol Fast Blue (LFB) staining and Masson staining were used for light microscopic observation.

Statistical analyses

DTI parameters were expressed by mean ± standard deviations. FA, ADC, AD and RD values between CCI and control groups were compared at each time point with the *t*-test. The changes in DTI parameters on each CCI and control side were tested using non-parametric one-way analysis of variance (ANOVA). Bonferroni test was performed to address of issue of multiple comparisons. Spearman's rank correlation coefficient was used to evaluate the correlation between DTI parameters and functional scores. All the analyses were performed by software package SPSS19.0 (Inc. Chicago, IL). A significance level of 0.05 was used for the statistical tests.

RESULTS

Morphology and signal changes on routine T_2 weighted sequence

On the T_2W/STIR images, both the sciatic nerves in each rabbit showed hyper-intense signals to adjacent muscles and symmetrical shape and course before CCI. After CCI, increased signal intensity and thickening were observed along the whole injured nerve. At the site of the injury, the nerve thickened like a spindle with blurry hyper-intense signals. With time, thickening of the nerve gradually localized and vanished, and signal intensity decreased as well. After 4 weeks post-injury, regional thickening almost disappeared, and the signal intensity of the injured nerve was mildly higher than its counterpart. After 10 weeks post-injury, signal intensity of the whole nerve was similar to normal, with only the injured portion being slightly lower in signal intensity than normal (Figure 2).

Quantitative changes of DTI parameters

The FA, ADC, AD and RD values are summarized in Table 1 and the corresponding time courses are shown in Figure 3.

Comparing DTI parameters at each time point on the CCI side, the FA value from day 3 to week 10 post-injury demonstrated significant decrease, compared to the pre-surgery baseline ($p < 0.006$ after Bonferroni correction). The FA value from

Figure 2. Serial images of T_2WI/STIR sequence at each time point after sciatic nerve constriction injury (CCI). Increased signal intensity along the nerve and local thickening were observed after 3 days post-injury. Signal intensity and thickness of injured nerve gradually decreased from 1 week to 4 weeks post-injury. After 4 weeks, the injured nerve showed a signal only a little higher in intensity than the counterpart. CCI, chronic constriction injuries; STIR, short-time inversion recovery; T_2WI, T_2 weighted.

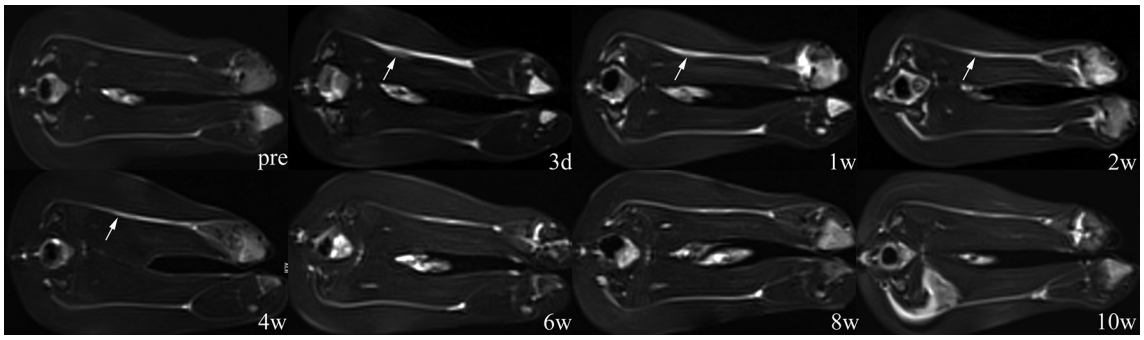

weeks 1 to 10 increased gradually, and there was no significant difference of FA between any adjacent time points. The ADC value significantly increased from day 3 to week 2 post-injury, compared to the baseline ($p < 0.006$ after Bonferroni correction). There was no significant difference of ADC between any adjacent time points except for ADC at weeks 2 and 4. The AD value showed significant decrease at day 3 days to 10 weeks, compared with baseline ($p < 0.006$ after Bonferroni correction). No variation trend of AD value was observed and no significant difference between any adjacent time points was found. The RD value significantly increased from day 3 to week 2 post-injury, compared to the baseline ($p < 0.006$ after Bonferroni correction). There was no significant difference in the RD value between any adjacent time points except for ADC at weeks 2 and 4. In contrast, there is no significant difference in the DTI parameters between the pre-surgery baseline and the sham-operated controls.

As shown in Figure 3, all the DTI parameters on the CCI side demonstrated significant difference from the control side at multiple time points. The FA value decreased sharply on day 3 and increased gradually from week 1 week to week 10 post-injury, but was significantly lower than the controls ($p < 0.006$ after Bonferroni correction). The ADC value increased significantly from day 3 to week 2, compared to the controls ($p < 0.006$ after Bonferroni correction). At week 4, the ADC value began to decrease, and there was no significant difference compared to the controls. The AD value decreased on day 3, and remained significant lower than the controls from day 3 to week 10 ($p < 0.006$ after Bonferroni correction). The RD value increased sharply on day 3, and decreased gradually from day 3 to week 10, which remained significantly higher than the controls ($p < 0.006$ after Bonferroni correction).

Morphological changes on DTT

The sciatic nerves disintegrated at the site of CCI on day 3. At week 1, the integration of nerve fibres still existed, but the space between the distal and proximal ends of fibres narrowed. At week 2 the fibre bundles mostly reappeared and passed through the CCI section, and reconnected with the distant fibres. From weeks 4 to 10, the nerves looked the same as the control side in terms of length and thickness (Figure 4).

Table 1. DTI parameters in the CCI group of sciatic nerves

Time points	FA	ADC (×10−3 mm^2 s^{-1})	AD	RD
Baseline	0.573 ± 0.035	1.305 ± 0.049	2.317 ± 0.118	0.799 ± 0.066
3d	0.316 ± 0.044[a]	1.502 ± 0.126*	2.042 ± 0.160[a]	1.233 ± 0.152[a]
1w	0.331 ± 0.018[a]	1.462 ± 0.058*	2.005 ± 0.095[a]	1.190 ± 0.060[a]
2w	0.354 ± 0.044[a]	1.473 ± 0.124*	2.057 ± 0.124[a]	1.181 ± 0.140[a]
4w	0.375 ± 0.015[a]	1.356 ± 0.129	1.952 ± 0.213[a]	1.071 ± 0.102[a]
6w	0.394 ± 0.020[a]	1.375 ± 0.107	1.988 ± 0.180[a]	1.068 ± 0.084[a]
8w	0.420 ± 0.031[a]	1.290 ± 0.064	1.947 ± 0.106[a]	0.961 ± 0.063[a]
10w	0.464 ± 0.039[a]	1.298 ± 0.026	2.097 ± 0.114[a]	0.923 ± 0.058[a]
F	51.319	5.298	4.305	15.798
P	0.000	0.000	0.001	0.000

Non-parametric one-way analysis of variance (ANOVA) was used for the changes of DTI parameters at each time point. Data are the means 3 standard deviations.

AD, axial diffusivity; ADC, apparent diffusion coefficient; d, day; FA, fractional anisotropy; RD, radial diffusivity; w, month.

[a]$p < 0.006$, after Bonferroni correction, compared to the baseline.

Figure 3. Time courses of FA, ADC, AD and RD values for both CCI and sham-operation groups. The ADC values are in $\times 10^{-3}$ mm^2 s^{-1}. *$p < 0.006$ with Bonferroni correction for between-group comparison.

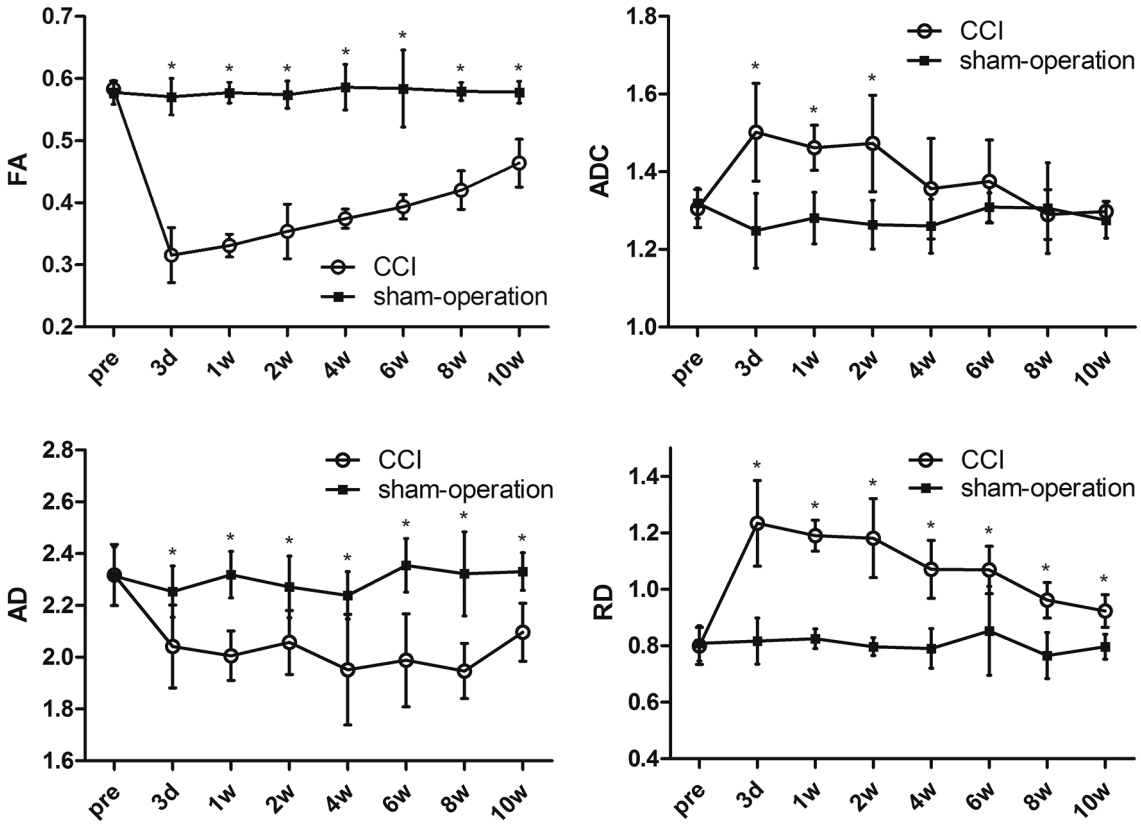

Correlation between limb function and DTI parameters

The limb function scores are summarized in Table 2 and the correlation between the DTI parameters and the function scores is shown in Figure 5. As shown in Table 2, the score totals decreased sharply at first and gradually recovered with time. Analysis on the correlation between the DTI parameters and limb function scores showed that the function scores were positively correlated with the FA value ($R = 0.805$, $p < 0.001$), and negatively with the ADC value and the RD value ($R = -0.55$, $p < 0.001$; $R = -0.744$, $p < 0.001$). However, no significant correlation was found between the limb function and the AD value ($R = 0.281$, $p = 0.053$).

Histological changes

Multiple staining methods were used to evaluate the histological changes of the axon, myelin sheath and interstitial substance of sciatic nerves. As shown in Figure 6, cross-sections of the normal nerve demonstrated densely-arranged, oval or polygon-like axons with uniform red staining and consistent size on H.E staining, and fence-like myelin sheath around the axon with blue staining on LFB staining, and thin epineurium and scarce collagenous fibres with blue staining on Masson staining.

During the 10 week follow-up, the main pathological presentation of the injured nerve was as follows. The changes of myelin sheath included swelling and loosening of the structure (day 3 to

Figure 4. Serial changes of the nerve bundles on DTT. The injured nerve bundles showed disruption at 3 days after injury. The disruption is an artefact that was caused by FA decreases resulted by swelling and oedema. At 1 week post-injury, the proximate and distant ends of the nerve bundles showed to get closer to each other. After 2 weeks post-injury, the injured nerve bundles seemed the same to the counterparts. (Images at the later time points were not shown here). DTT, diffusion tensor tractography; FA, fractional anisotropy.

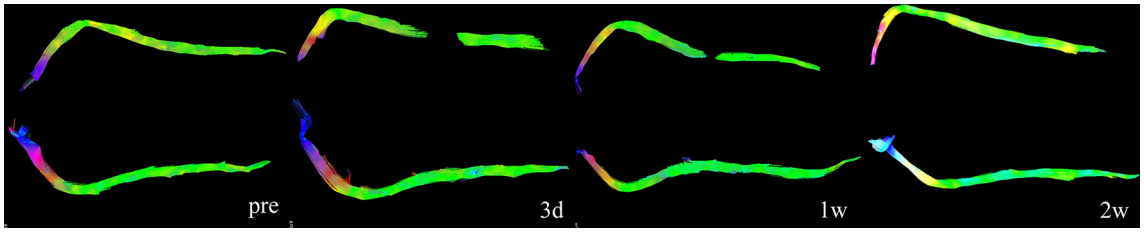

Table 2. Function scores of limbs with CCI

Time points	Toe-spreading reflex				Response to acupuncture				Resistance to hand press				Gait			Total score
	1	2	3	4	1	2	3	4	1	2	3	4	1	2	3	
Baseline	0	0	0	6	0	0	0	6	0	0	0	6	0	0	6	90
3d	5	1	0	0	5	1	0	0	5	1	0	0	5	1	0	28
1w	6	0	0	0	4	2	0	0	5	1	0	0	3	3	0	30
2w	5	0	1	0	4	2	0	0	2	4	0	0	0	6	0	38
4w	2	1	3	0	1	4	1	0	0	3	3	0	0	2	4	56
6w	0	1	1	4	1	2	2	1	0	1	5	0	0	1	5	70
8w	0	1	1	4	1	1	2	2	0	1	2	3	0	1	5	75
10w	0	1	0	5	0	1	3	2	0	0	3	3	0	1	5	79

CCI, chronic constriction injury.

week 1), breaking down and demyelination (weeks 2 to 4), regeneration and maturation (weeks 4 to 10). The changes of nerve fibres consisted of transformation from myelinated fibres to swollen fibres (day 3 to week 2) and replacement of the swollen fibres by regenerated, thinly myelinated fibres (weeks 4 to 10). Besides, there were infiltration of acute inflammatory cells and tissue oedema at the early stage (day 3 to week 2) and proliferation of chronic inflammatory cells and epineural fibrosis and endoneural fibrosis at delayed stage (weeks 4 to 10) (Figure 6).

DISCUSSION

Compressive nerve injury is a multiphase pathological process, and there are distinctive features between acute and chronic injuries. In previous studies, acute crush and traction injuries were established to mimic the degeneration and regeneration of peripheral nerves. The injuries induced sudden damages to the nerves, leading to rapid demyelination and axonal loss, and release of the crush or traction was followed by natural regeneration of the nerve fibres.[12–14,17,18] In addition, a series of animal experiments were conducted by Roger Gilliat to study the pathological changes of the distal nerve due to a proximal nerve ligation, and it has been confirmed that a persistent tight constricting ligature on the peripheral nerve causes Wallerian degeneration and functional disorders of the distal nerve.[19,20] In our study, the CCI model was different from those above because it was neither a sudden damage nor a tight ligation. Instead, we used a series of loose constrictive ligation around the nerve to establish alien stimulation, regionally increased pressure and blood flow obstruction, possibly major factors that originated the NCS. Therefore, we believe it started a chronic process that contained relatively comprehensive pathological changes.

A recent longitudinal study on amyotrophic lateral sclerosis (ALS) concluded that AD decreases may be caused by axonal degeneration, such as the effects of axon fragmentation and accumulation of cell debris.[21] However, in our study, the AD value was still lower than the normal after the axonal regeneration, and we think the decreases may be partly due to nerve fibrosis. Additionally, a few studies explored changes in the DTI parameters in relation to peripheral nerves in ALS patients and concluded that the decreases in FA and AD values were associated with axonal injuries and that pathological changes in the peripheral nerves were associated with axonal degeneration and demyelination while chronic nerve fibrosis might also contribute to the decreases in AD values.[22,23]

We observed that establishment of the CCI model was followed by a series of pathologic changes. In the acute stage, intra- and extraneural oedema, inflammation and fibrin deposits were the main changes within the compressed nerves, which were probably induced by increased vascular permeability of the epineural and endoneural vessels after compression. In the delayed stage, despite the persisting ischaemia, nutrient supplies were partially restored as endoneural fibroblasts and capillary endothelial cells started to proliferate, and demyelination and axonal degeneration were observed along the compressed fascicles. These phenomena are perhaps the underlying reasons for partial self-regeneration of the constricted nerves. In the end, chronic

Figure 5. Correlation between functional assessment and DTI parameters including FA, ADC and RD values. In the injured nerves, FA was positively correlated with function scores while ADC and RD, negatively.

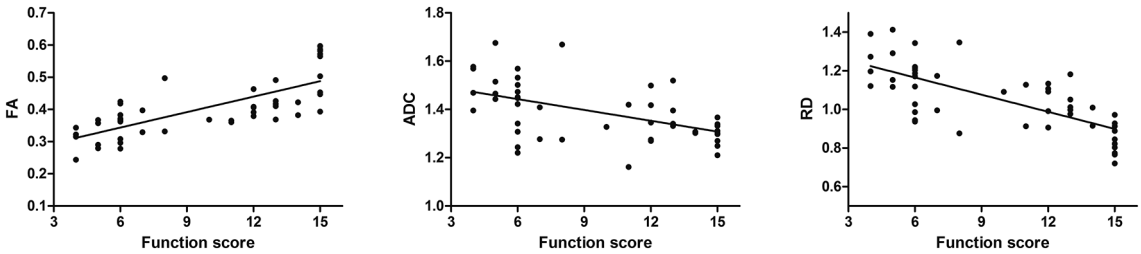

nerve compression is associated with connective tissue changes including epineural fibrosis, perineural thickening, and ultimately endoneurial fibrosis.[1,2,15] Therefore, the axonal injury was not caused by the CCI model itself, but regional blood obstruction and demyelination led to axonal degeneration. However, the degeneration was not simply neuropraxic, but accompanied by neural fibrosis due to external stimulus.[24] In addition, it is noteworthy to point out that the disconnection of neural fibres at the site of injury, observed in this study, did not really indicate disruption of the nerve. Based on the principles of DTT and the threshold of FA = 0.3 in our study, the disruption was observed when FA of local fibres was lower than 0.3. It was therefore an artefact in the study that disturbed the mathematical algorithm underlying the creation of tractography images. Furthermore, different from previous studies on acute injuries, the CCI model here introduced a gradual progression of neural changes, and the Wallerian degeneration with loss of distal axons, commonly seen in acute models, was not observed here.

To our knowledge, no DTI studies on chronic compressive nerve injury were performed to explore the association of DTI parameters and pathological changes and motor function. In this study, CCI was chosen as the model for chronic compressive nerve injury, and the serial inflammatory reactions of the nerves subjected to CCI were reflected by various changes of different DTI parameters, which indicated that the DTI parameters could be used to detect and monitor the acute and chronic changes after nerve compression.

The feasibility of DTI in evaluating acute mechanical injuries and radiation-induced injuries of peripheral nerves has been explored by previous studies, and good correlation between DTI

Figure 6. Serial histological changes of the injured nerves with HE staining (1st row), LFB staining (2nd row) and Masson staining (3rd row). Proliferation of inflammatory cells, oedema and swelling occurred at 3 days post-injury. The myelinated nerve fibres began to break down at 3 days post-injury and thinly myelinated fibres gradually proliferated since 6 weeks post-injury. The thickening and fibrosis of epineurium and perineurium started at 4 weeks post-injury and progressed during the observation period. HE, haematoxylin–eosin; LFB, Luxol Fast Blue.

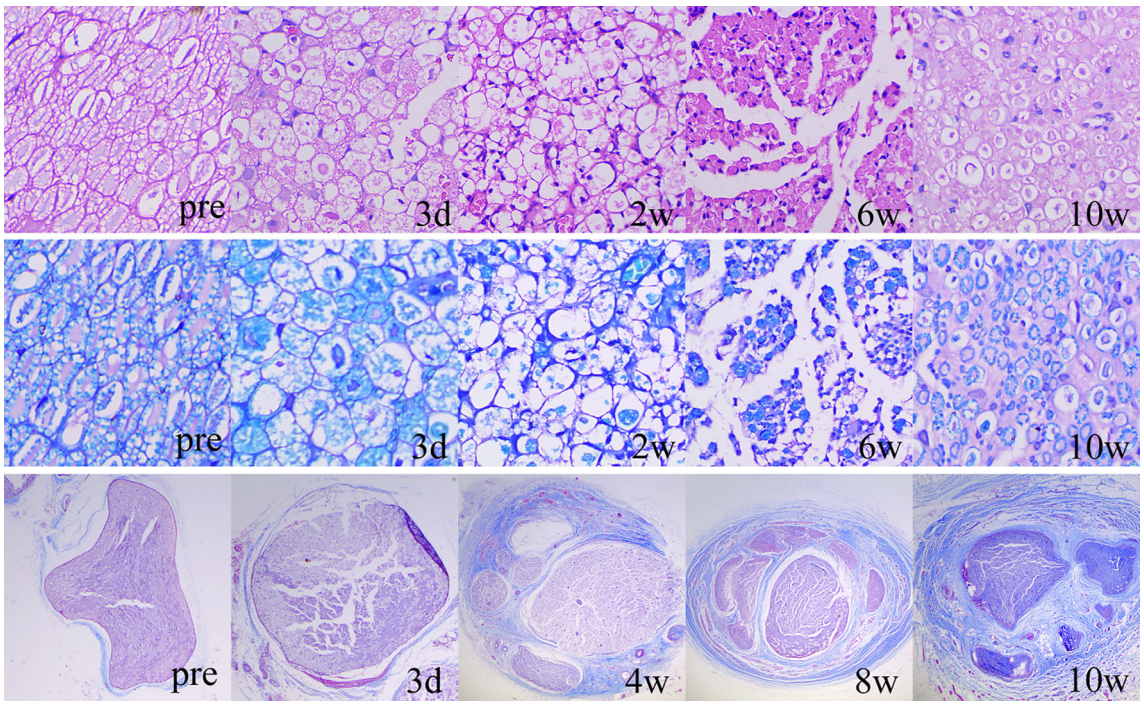

parameters and limb function, as well as pathological changes, were reported.[14,18,25,26] A significant decrease of limb function right after injury and a gradual recovery were observed in both crush and traction injuries, and it was positively correlated with the FA value and negatively with RD.[12,13] Among these studies, which were all based on animal models, Tarlov scores and toe-spreading reflex were commonly used in assessing limbs. With similar methods, our results were in accordance to the previous studies by showing similar correlation between the DTI parameters and limb functions. In addition, a few studies[14,17,18] analysed histological changes of injured nerves using quantitative metrics for axons and myelin sheath and evaluated the correlation between these metrics and the DTI parameters. The results demonstrated that FA changes were positively correlated with axon number (density) and negatively with myelin sheath thickness. Besides, pathology and DTI parameters were compared in a couple of studies and FA and RD values were found to be consistent with the pathological changes with time.[13,25] Therefore, alteration of the DTI parameters, especially FA, can mainly be attributed to the alteration of axons and myelin sheath.

Aside from the changes of FA, we also found increased ADC value from day 3 to week 2 and decreased AD value during the whole period of observation, which were not shown in earlier animal studies. In clinical studies on NCS, however, the rise of ADC value was frequently reported[19, 20], and the alteration of ADC correlated with nerve conduction velocity (NCV) and electromyography (EMG) measurements.[9,27] Furthermore, Naraghi et al[28] found that the ADC value of the median nerve in CTS patients recovered after carpal tunnel release. Hiltunen et al[8] by monitoring pre- and post-operative DTI parameters, realized that the clinical improvement of CTS patients was reflected in diffusivity such as the value of mean diffusivity (MD), but not in anisotropy such as FA. In these clinical studies, inflammation, oedema and swelling of nerves were thought to contribute to the increase of the ADC (MD) value. Our results supported this speculation by showing the increase of ADC coupled with swelling of axons and myelin sheath. Also found here was the significant correlation between limb function and ADC. However, in our experiment, the ADC value decreased after 2 weeks post-injury, indicating that other pathological changes, such as epineural and endoneural fibrosis that were observed in this study, played a role in influencing the diffusivity of peripheral nerves. In addition, our results demonstrated a descending trend of the ADC value, consistent with the significant decrease of ADC shown in previous studies. Therefore, we hypothesized that the rise of ADC reflected oedema and swelling of the nerve, while the reduction of it was related to the development of fibrotic tissues in and around the nerve. Though it's been suggested that scar tissues may hinder the free diffusion of water and thus reduce ADC, it is still to be confirmed in further longitudinal DTI studies in animal models.

The reduction of the AD value within the injured peripheral nerve found in this study, although seldom reported, made it a promising biomarker for chronic injury to peripheral nerves. Lindberg et al[11] carried out a DTI study on recurrent CTS and found that DTI parameters including ADC, AD and RD values decreased along the median nerve in patients compared with controls. They suggested that the reduction of diffusivity was related to endoneural fibrosis and slower nerve conduction. The AD value reflects water diffusion along the nerve and provides information about the integrity of axons. In our CCI model, nerve bundles were constricted by four silk sutures. It is thus possible that AD decreased at the beginning of the injury because the constriction limited the parallel diffusion of axoplasm and blood perfusion.[24] In the delayed phase, the persistence of constriction and development of epineural and endoneural fibrosis kept the AD value of nerve fascicles low throughout observation. In contrast, in acute injury models, nerve bundles are so severely disrupted that the microstructure including axons and myelin sheath break down soon after injury. Such disruption lifts some restriction away from the radial diffusion of water molecules, as reflected by the increase of RD values, but has little effect on AD since the axial diffusion is rarely affected.[12,13]

Previous DTI studies on degeneration and regeneration of peripheral nerves suggested that DTT could be used to determine the tracks of nerve fibres.[17,18,29] Our results were consistent with the findings by showing separation of proximate and distant parts of nerve fibres on day 3 and week 1 post-injury. Nevertheless, the axon loss was not as severe as what had been expected for the acute stage of CCI. Not until 4 weeks post-injury did the axon number reach the lowest in our experiment. Furthermore, the post-processing of DTT is based on the FA value that can be influenced by multiple pathological changes which, in nerves with CCI, are more than just axon loss and demyelination and also include anisotropy of water diffusion, such as swelling and fibrosis. Therefore, we concluded that DTT might not be a suitable method for evaluating nerve fibres in the CCI model, although it is not a quantitative method.

CCI is a classical animal model that is widely used to induce neuropathic pain. This model is commonly produced on rodents such as rats and mice.[30,31] In the present study, rabbits were used because their larger size made it easier for neural imaging. Although several other methods were introduced to produce chronic compression on peripheral nerves, CCI using silk suture was chosen for the following reasons. Firstly, the constriction with silk suture is a proper way to mimic clinical conditions like mechanical compression on nerves within tunnel and local nerve adhesion by fibrous tissue. Secondly, based on our pathological follow-ups, CCI provides us with various characteristics of injured nerves at different pathological stages including swelling, axon loss and demyelination, and intraneural fibrosis. Finally, compared with tube of silicone, polyethylene and metal clamps, silk suture minimizes the influence of alien material on DT imaging and metrics measurement. Therefore, we believe that CCI is a suitable model to study chronic nerve compression with DTI.

We chose rabbits in the study because they were bigger than rodents and the size of their sciatic nerves was able to meet the requirements of DTI and 3T imaging, leading to future studies on patients and clinical applications. More complicated techniques such NODDI, DSI and DKI may help researchers obtain more

details on nerve microstructure based on various modeling and algorithms. However, NODDI and DSI, with wide application in brain imaging, may only be useful in a few complex peripheral nerves such as lumbosacral plexus and brachial plexus while over-qualified in most peripheral nerves with simple structures. In addition, peripheral nerves are usually buried among complex tissues and it can be difficult to get high-quality images through the techniques above. In contrast, DKI and IVIM-DWI report signal diffusion within a tissue, and may be applied in peripheral nerve diseases such as tumours and inflammation, but the efficacy of the techniques relies heavily on resolution and post-imaging management techniques.

There are some limitations to this study. First, the DTI monitoring period of CCI was just 10 weeks. Although the progression of epineural and perineural fibrosis was observed during this period, additional studies on CCI with longer observational duration are needed to explore how further aggravated fibrosis influences DTI parameters. Second, quantitative methods were not used in the pathological evaluation, and there lacked electrophysiological evidence. Therefore, the exact correlation between pathological changes (including swelling, axon loss, demyelination, and fibrosis) and DTI parameters in the CCI model is to be revealed in future studies. Furthermore, the cross-sectional area is not known. Although measuring the area using existing images is possible, it was not suitable here. The CCI model here covered multiple pathological changes, and one focus of this study was to explore the effects of these changes, especially fibrosis, on the DTT parameters. Therefore, a simple calculation of the cross-sectional area could not reflect the changes in the CCI model. We expect to employ effective methods, such as analysing relevant proteins, to quantitate the changes of the nerves including the cross-sectional area in future studies. Thirdly, the present study indicates that diffusivity and anisotropy reflected by DTI are limited to distinguishing the multiple pathological changes in chronic nerve compression. Further exploration using advanced DWI-derived sequences such as IVIM-DWI, DKI and DSI may provide us with more details in the nerve alteration during compression. Last but not the least, the study found association, but not causation between DTI parameters in evaluating NCS, and more efforts are needed to uncover the pathological causes of the injuries.

CONCLUSION

In summary, CCI is a suitable model for DTI study on NCS. DTI parameters show distinguished changing pattern in monitoring peripheral nerves with CCI. The FA value is positively correlated with limb function, and ADC and RD values are negatively correlated with limb function, suggesting that FA, ADC and RD may be used to monitor chronic nerve injuries. The AD value is stably decreased during observation, suggesting that decreased AD may be an accurate biomarker for chronic injury to peripheral nerves. The alteration of DTI parameters is associated with multiple pathological changes such as nerve swelling, axon loss, demyelination and nerve fibrosis. Among them, FA and RD may be mostly influenced by axon degeneration and demyelination, increased ADC may be attributed to oedema and swelling, and decreased AD, mainly to constriction and fibrosis. In conclusion, DTI is a promising method in evaluating chronic nerve compression.

FUNDING

The study was supported by two grants from Natural Science Fund of Hubei Province in 2017 (2017CFB708 and 2017CFB644) and one from Innovative Research Fund of Huazhong University of Science and Technology in 2016 (2016YXMS234).

REFERENCES

1. Robinson LR. Traumatic injury to peripheral nerves. *Muscle Nerve* 2000; **23**: 863–73. doi: https://doi.org/10.1002/(SICI)1097-4598(200006)23:6<;863::AID-MUS4>;3.0.CO;2-0
2. Diao E, Andrews A, Diao J. Animal models of peripheral nerve injury. *Oper Tech Orthop* 2004; **14**: 153–62. doi: https://doi.org/10.1053/j.oto.2004.08.003
3. Meijboom R, Steketee RM, de Koning I, Osse RJ, Jiskoot LC, de Jong FJ, et al. Functional connectivity and microstructural white matter changes in phenocopy frontotemporal dementia. *Eur Radiol* 2017; **27**. Epub 2016/07/21. doi: https://doi.org/10.1007/s00330-016-4490-4
4. Lindberg PG, Sanchez K, Ozcan F, Rannou F, Poiraudeau S, Feydy A, et al. Correlation of force control with regional spinal DTI in patients with cervical spondylosis without signs of spinal cord injury on conventional MRI. *Eur Radiol* 2016; **26**: 733–42. Epub 2015/07/01. doi: https://doi.org/10.1007/s00330-015-3876-z
5. Naraghi AM, Awdeh H, Wadhwa V, Andreisek G, Chhabra A. Diffusion tensor imaging of peripheral nerves. *Semin Musculoskelet Radiol* 2015; **19**: 191–200. doi: https://doi.org/10.1055/s-0035-1546824
6. Simon NG, Lagopoulos J, Gallagher T, Kliot M, Kiernan MC. Peripheral nerve diffusion tensor imaging is reliable and reproducible. *J Magn Reson Imaging* 2016; **43**: 962–9. doi: https://doi.org/10.1002/jmri.25056
7. Stein D, Neufeld A, Pasternak O, Graif M, Patish H, Schwimmer E, et al. Diffusion tensor imaging of the median nerve in healthy and carpal tunnel syndrome subjects. *J Magn Reson Imaging* 2009; **29**: 657–62. doi: https://doi.org/10.1002/jmri.21553
8. Hiltunen J, Kirveskari E, Numminen J, Lindfors N, Göransson H, Hari R. Pre- and post-operative diffusion tensor imaging of the median nerve in carpal tunnel syndrome. *Eur Radiol* 2012; **22**: 1310–9. doi: https://doi.org/10.1007/s00330-012-2381-x
9. Wang CK, Jou IM, Huang HW, Chen PY, Tsai HM, Liu YS, et al. Carpal tunnel syndrome assessed with diffusion tensor imaging: comparison with electrophysiological studies of patients and healthy volunteers. *Eur J Radiol* 2012; **81**: 3378–83. Epub 2012/02/03. doi: https://doi.org/10.1016/j.ejrad.2012.01.008
10. Kwon BC, Koh SH, Hwang SY. Optimal parameters and location for diffusion-tensor imaging in the diagnosis of carpal tunnel syndrome: a prospective matched case-control study. *AJR Am J Roentgenol* 2015; **204**: 1248–54. doi: https://doi.org/10.2214/AJR.14.13371

11. Lindberg PG, Feydy A, Le Viet D, Maier MA, Drapé JL. Diffusion tensor imaging of the median nerve in recurrent carpal tunnel syndrome - initial experience. *Eur Radiol* 2013; **23**: 3115–23. doi: https://doi.org/10.1007/s00330-013-2986-8
12. Yamasaki T, Fujiwara H, Oda R, Mikami Y, Ikeda T, Nagae M, et al. In vivo evaluation of rabbit sciatic nerve regeneration with diffusion tensor imaging (DTI): correlations with histology and behavior. *Magn Reson Imaging* 2015; **33**: 95–101. doi: https://doi.org/10.1016/j.mri.2014.09.005
13. Li X, Chen J, Hong G, Sun C, Wu X, Peng MJ, et al. In vivo DTI longitudinal measurements of acute sciatic nerve traction injury and the association with pathological and functional changes. *Eur J Radiol* 2013; **82**: e707–14e714. Epub 2013/08/21. doi: https://doi.org/10.1016/j.ejrad.2013.07.018
14. Boyer RB, Kelm ND, Riley DC, Sexton KW, Pollins AC, Shack RB, et al. 4.7-T diffusion tensor imaging of acute traumatic peripheral nerve injury. *Neurosurg Focus* 2015; **39**: E9. doi: https://doi.org/10.3171/2015.6.FOCUS1590
15. Bennett GJ, Xie YK. A peripheral mononeuropathy in rat that produces disorders of pain sensation like those seen in man. *Pain* 1988; **33**: 87–107. doi: https://doi.org/10.1016/0304-3959(88)90209-6
16. Wan Q, Wang S, Zhou J, Zou Q, Deng Y, Wang S, , et al. Evaluation of radiation-induced peripheral nerve injury in rabbits with MR neurography using diffusion tensor imaging and T_2 measurements: Correlation with histological and functional changes. *J Magn Reson Imaging* 2016; **43**: 1492–9. Epub 2015/12/23. doi: https://doi.org/10.1002/jmri.25114
17. Lehmann HC, Zhang J, Mori S, Sheikh KA. Diffusion tensor imaging to assess axonal regeneration in peripheral nerves. *Exp Neurol* 2010; **223**: 238–44. doi: https://doi.org/10.1016/j.expneurol.2009.10.012
18. Takagi T, Nakamura M, Yamada M, Hikishima K, Momoshima S, Fujiyoshi K, et al. Visualization of peripheral nerve degeneration and regeneration: monitoring with diffusion tensor tractography. *Neuroimage* 2009; **44**: 884–92. doi: https://doi.org/10.1016/j.neuroimage.2008.09.022
19. Shimpo T, Gilliatt RW, Kennett RP, Allen PJ. Susceptibility to pressure neuropathy distal to a constricting ligature in the guinea-pig. *J Neurol Neurosurg Psychiatry* 1987; **50**: 1625–32. doi: https://doi.org/10.1136/jnnp.50.12.1625
20. Reiners K, Gilliatt RW, Harding AE, O'Neill JH. Regeneration following tibial nerve crush in the rabbit: the effect of proximal constriction. *J Neurol Neurosurg Psychiatry* 1987; **50**: 6–11. doi: https://doi.org/10.1136/jnnp.50.1.6
21. Marcuzzo S, Bonanno S, Figini M, Scotti A, Zucca I, Minati L, et al. A longitudinal DTI and histological study of the spinal cord reveals early pathological alterations in G93A-SOD1 mouse model of amyotrophic lateral sclerosis. *Exp Neurol* 2017; **293**: 43–52. Epub 2017/03/30. doi: https://doi.org/10.1016/j.expneurol.2017.03.018
22. Simon NG, Lagopoulos J, Paling S, Pfluger C, Park SB, Howells J, et al. Peripheral nerve diffusion tensor imaging as a measure of disease progression in ALS. *J Neurol* 2017; **264**: 882–90. Epub 2017/03/08. doi: https://doi.org/10.1007/s00415-017-8443-x
23. Haakma W, Jongbloed BA, Froeling M, Goedee HS, Bos C, Leemans A, et al. MRI shows thickening and altered diffusion in the median and ulnar nerves in multifocal motor neuropathy. *Eur Radiol* 2017; **27**: 2216–24. Epub 2016/09/23. doi: https://doi.org/10.1007/s00330-016-4575-0
24. Fischer-Hayes LR, Brotherton T, Glass JD. Axonal degeneration in the peripheral nervous system: implications for the pathogenesis of amyotrophic lateral sclerosis. *Exp Neurol* 2013; **246**: 6–13. doi: https://doi.org/10.1016/j.expneurol.2013.05.001
25. Wan Q, Wang S, Zhou J, Zou Q, Deng Y, Wang S, et al. Evaluation of radiation-induced peripheral nerve injury in rabbits with MR neurography using diffusion tensor imaging and T_2 measurements: correlation with histological and functional changes. *J Magn Reson Imaging* 2016; **43**: 1492–9. doi: https://doi.org/10.1002/jmri.25114
26. Yayama T, Kobayashi S, Nakanishi Y, Uchida K, Kokubo Y, Miyazaki T, et al. Effects of graded mechanical compression of rabbit sciatic nerve on nerve blood flow and electrophysiological properties. *J Clin Neurosci* 2010; **17**: 501–5. doi: https://doi.org/10.1016/j.jocn.2009.07.110
27. Bulut HT, Yildirim A, Ekmekci B, Gunbey HP. The diagnostic and grading value of diffusion tensor imaging in patients with carpal tunnel syndrome. *Acad Radiol* 2014; **21**: 767–73. doi: https://doi.org/10.1016/j.acra.2014.02.009
28. Naraghi A, da Gama Lobo L, Menezes R, Khanna M, Sussman M, Anastakis D, et al. Diffusion tensor imaging of the median nerve before and after carpal tunnel release in patients with carpal tunnel syndrome: feasibility study. *Skeletal Radiol* 2013; **42**: 1403–12. doi: https://doi.org/10.1007/s00256-013-1670-z
29. Kabakci NT, Kovanlikaya A, Kovanlikaya I. Tractography of the median nerve. *Semin Musculoskelet Radiol* 2009; **13**: 018–23. doi: https://doi.org/10.1055/s-0029-1202241
30. Fei-E Z, Jun-Li C, Li-Cai Z, Yin-Ming Z. Activation of p38 mitogen-activated protein kinase in spinal cord contributes. *Acta Physiologica Sinica* 2005; **57**: 545–51.
31. Zanella JM, Burright EN, Hildebrand K, Hobot C, Cox M, Christoferson L, et al. Effect of etanercept, a tumor necrosis factor-alpha inhibitor, on neuropathic pain in the rat chronic constriction injury model. *Spine* 2008; **33**: 227–34. doi: https://doi.org/10.1097/BRS.0b013e318162340a